16. O. Legasa, A. D. Buscalioni, Z. Gasparini, *Stud. Geol. Salm.* **29**, 127 (1994).
17. Materials and methods are available as supporting material on *Science* Online.
18. The phylogenetic data set included 257 characters scored across 58 crocodylomorph taxa at the species level, expanding previously published data sets (*27*), and was analyzed using parsimony in TNT v.1.0 (*28*). See (*17*) for further details.
19. S. Hua, V. de Buffrenil, *J. Vertebr. Paleontol.* **16**, 703 (1996).
20. M. Fernández, Z. Gasparini, *Lethaia* **33**, 269 (2000).
21. G. A. Buckley, C. A. Brochu, D. W. Krause, D. Pol, *Nature* **405**, 941 (2000).
22. N. N. Iordansky, in *The Biology of Reptilia* 4, C. Gans, T. Parsons, Eds. (Academic Press, New York, 1973), pp. 201–262.
23. C. A. Brochu, *Am. Zool.* **41**, 564 (2001).
24. S. Jouve, B. Bouya, M. Amaghzaz, *Palaeontology* **48**, 359 (2005).
25. M. Delfino, P. Piras, T. Smith, *Acta Palaeontol. Pol.* **50**, 565 (2005).
26. D. M. Martill, *Neues Jahrb. Geol. Palaeontol. Monatsh.* **1986**, 621 (1986).
27. D. Pol, M. A. Norell, *Am. Mus. Novit.* **3458**, 1 (2004).
28. P. A. Goloboff, J. S. Farris, K. Nixon, TNT ver. 1.0. Program and documentation available from the authors and at www.zmuc.dk/public/phylogeny (2003).
29. P. A. Goloboff, C. I. Mattoni, A. S. Quinteros, *Cladistics* **20**, 595 (2004).
30. The specimens reported here were found by S. Cocca and R. Cocca from the Museo Olsacher (Dirección de Minería, Neuquén Province, Argentina) and prepared by J. Moly (Museo de La Plata). Scanning electron microscope images were taken by R. Urréjola. Drawings for Figs. 1 to 3 were executed by Jorge González. We thank S. Jouve, S. Hwang,

The Late Miocene Radiation of Modern Felidae: A Genetic Assessment

Warren E. Johnson,[1]* Eduardo Eizirik,[1,2] Jill Pecon-Slattery,[1] William J. Murphy,[1]† Agostinho Antunes,[1,3] Emma Teeling,[1]‡ Stephen J. O'Brien[1]*

Modern felid species descend from relatively recent (<11 million years ago) divergence and speciation events that produced successful predatory carnivores worldwide but that have confounded taxonomic classifications. A highly resolved molecular phylogeny with divergence dates for all living cat species, derived from autosomal, X-linked, Y-linked, and mitochondrial gene segments (22,789 base pairs) and 16 fossil calibrations define eight principal lineages produced through at least 10 intercontinental migrations facilitated by sea-level fluctuations. A ghost lineage analysis indicates that available felid fossils underestimate (i.e., unrepresented basal branch length) first occurrence by an average of 76%, revealing a low representation of felid lineages in paleontological remains. The phylogenetic performance of distinct gene classes showed that Y-chromosome segments are appreciably more informative than mitochondrial DNA, X-linked, or autosomal genes in resolving the rapid Felidae species radiation.

The first felidlike carnivores appeared in the Oligocene, approximately 35 million years ago (Ma). Living cat species (subfamily Felinae) originated in the late Miocene and evolved into one of the world's most successful carnivore families, inhabiting all the continents except Antarctica (*1*, *2*). Understanding their evolutionary history and establishing a consensus taxonomic nomenclature has been complicated by rapid and very recent speciation events, few distinguishing dental and skeletal characteristics, incidents of parallel evolution, and an incomplete fossil record (*1*–*5*). Recent analyses (*6*–*8*) identified eight major felid lineages, although their chronology, branching order, and exact composition remained unresolved (*4*–*8*). Here, we present an analysis of DNA sequence from 19 independent autosomal (aDNA), five X-linked (xDNA), six Y-linked (yDNA), and nine mitochondrial (mtDNA) gene segments (tables S1 to S3) sampled across the 37 living felid species plus 7 outgroup species representing each feliform carnivoran family (*9*).

We present a phylogenetic analysis (Fig. 1) for nuclear genes (nDNA) [combined y, x, and aDNA = 18,853 base pairs (bp)] that leads to several conclusions. First, the eight Felidae lineages are strongly supported by bootstrap analyses and Bayesian posterior probabilities (BPP) for the nDNA data and most of the other separate gene partitions (Table 1 and figs. S1 to S11), by rare shared derived indels, including endogenous retroviral families in the domestic cat lineage (*10*), by transposed nuclear mtDNA sequences (*Numt*) in the domestic cat (node 9) and *Panthera* lineages (node 33) (*11*, *12*) (Table 1 and table S7), by 11 to 65 diagnostic sites for individual lineages (tables S5 and S8), and by amino acid data analyses of 14 genes (1457 sites) (tables S9 and S10 and fig. S1). Second, the four species previously unassigned to any lineage (marbled cat, serval, pallas cat, and rusty spotted cat) (*6*) have now been confidently placed. Third, the hierarchy and timing of divergences among the eight lineages are clarified (Fig. 1 and Table 1). Fourth, the phylogenetic relationships among the nonfelid species of hyenas, mongoose, civets, and linsang corroborate previous inferences with strong support (*13*, *14*).

The radiation of modern felids began with the divergence of the *Panthera* lineage leading to the clouded leopard and the "great roaring cats" of the *Panthera* genus (node 33 in Fig. 1). Support for this basal position was strong (88 to 100%) with all analytic methods and gene partitions (Table 1 and table S4) contrasting with some previous results that suggested a more internal position for the big cats (*7*). The split of the *Panthera* lineage was followed by a rapid progression of divergence events. The first led to the bay cat lineage, a modern assemblage of three Asian species (bay cat, marbled cat, and Asian golden cat) (node 31), followed by divergences of the caracal lineage, with three modern African species (caracal, serval, and African golden cat) (node 29) and of the ocelot lineage (node 23), consisting of seven Neotropical species. Bootstrap support (BS) for the nodes that produced these three early divergences (nodes 2 to 4) was moderate (74 to 97% nDNA BS) relative to nodes defining lineage groups (23, 29, and 31) with 100% nDNA BS. A more recent clade, including four lineages (lynx, puma, leopard cat, and domestic cat lineages) (node 5), is well supported (97 to 99% nDNA BS). The divergence of the lynx lineage was followed very closely by the appearance of the puma lineage (Fig. 1). However, these two North American groups were united as sister groups in some analyses using different data partitions and phylogenetic algorithms (figs. S6 to S11 and

[1]Laboratory of Genomic Diversity, National Cancer Institute, Frederick, MD 21702–1201, USA. [2]Centro de Biologia Genômica e Molecular, Faculdade de Biociências, Pontifícia Universidade Católica do Rio Grande do Sul, Avenida Ipiranga 6681, Porto Alegre, RS 90619-900, Brazil. [3]REQUIMTE, Departamento de Química, Faculdade de Ciências, Universidade do Porto, Rua do Campo Alegre, 687, 4169-007 Porto, Portugal.

*To whom correspondence should be addressed. E-mail: johnsonw@ncifcrf.gov (W.E.J.); obrien@ncifcrf.gov (S.J.O.)
†Present address: Department of Veterinary Integrative Biosciences, Texas A&M University, College Station, TX, 77843–4458, USA.
‡Present address: Department of Zoology, University College Dublin, Belfield, Dublin 4, Ireland.

Fig. 1. Phylogenetic relations among felid species and outgroup taxa depicted in a maximum likelihood tree [tree bisection-reconnection (TBR) search and general time reversible (GTR) + G + I model of sequence evolution from 18,853 bp of nDNA concatenated data] (9). Terminal nodes are labeled with three-letter codes, scientific name, and common name, and felid species are grouped into eight major lineages. Scientific names and branches are color coded to depict recent and historic zoogeographical regions (Oriental, Palearctic, Ethiopian, Neotropical, and Nearctic), as inferred from current distributions, fossil records, and our phylogenetic analyses (1–5, 9). Branches in black reflect either less certain historical interpretations or geographic distributions beyond one zoogeographic zone. Nodes 1 to 37 are numbered, and an asterisk indicates relatively low resolution (Table 1). Estimated divergence dates of lineage-defining nodes (1–7) are in red. Rare insertion/deletions supporting lineages as shared derived cladistic characters are indicated by an arrow (Table 1).
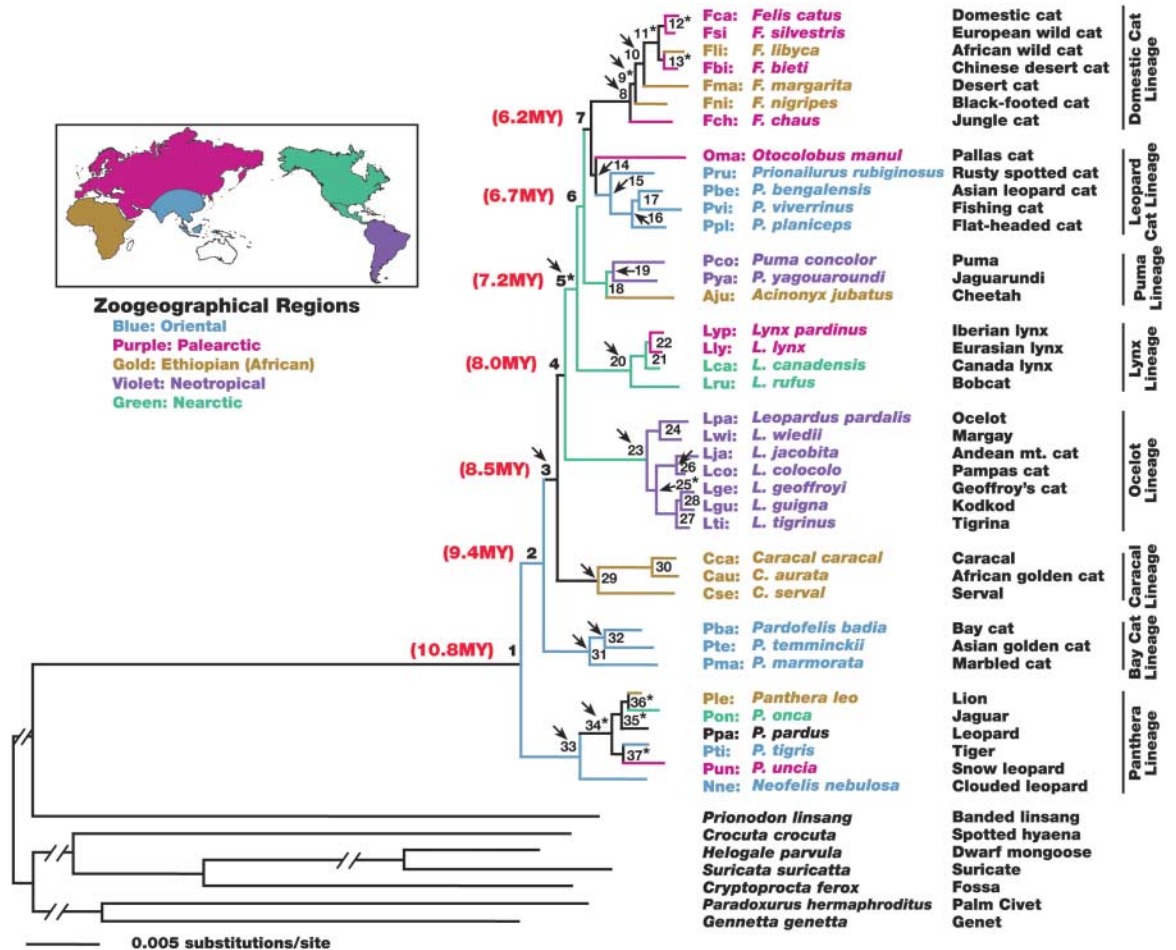
table S5). The two most recently derived groups were the domestic cat and leopard cat lineages (99 to 100% nDNA BS) (node 7). Support for inclusion of the pallas cat within the leopard cat lineage was moderate (76 to 100% nDNA BS) but included a single insertion/deletion (APP + 1) (Table 1 and table S7).

Together, each of the eight lineages received strong BS and BPP of 100% using nDNA, with slightly less support for the hierarchical intralineage relationships (Table 1). A few internal nodes with lower support must remain as uncertain (asterisk in Fig. 1), including the position of Andean mountain cat within the ocelot lineage, the branching order of jungle cat and black-footed cat within the domestic cat lineage, and the precise hierarchy among *Panthera* species. Support for these relations was low, probably as a result of inconsistent sorting patterns of ancestral polymorphisms. Even so, the overall support of the major nodes is strong, increasing confidence in the proposed topology (Fig. 1).

The earliest records of the Felinae are ascribed to late Miocene (~9 Ma) *Felis attica* fossils from western Eurasia (15). Estimates of divergence dates using a Bayesian approach

with 16 fossil calibration dates (9) indicate that the major felid lineages were established during a short evolutionary time period (10.8 to 6.2 Ma) (Fig. 1 and Table 1). Within-lineage divergences occurred during the late Miocene and early Pliocene (6.4 to 2.9 Ma), when sea levels were generally 90 to 100 m above modern levels (16). A second major surge in species differentiation followed from 3.1 to 0.7 Ma, with the initial appearance of 27 of 37 extant species that comprise modern felids (Fig. 1 and Table 1). These late Pliocene-Pleistocene species divergence episodes occurred during a period of relatively low sea levels before the onset of Pleistocene glacial oscillations (Fig. 2).

We propose a plausible biogeographic hypothesis of felid evolutionary history (Fig. 2) based on our results and geological events (16–19). The most parsimonious scenario implies that modern felids arose in Asia with the divergence of the *Panthera* lineage 10.8 Ma and, subsequently, the bay cat lineage 9.4 Ma. These dates correspond to extremely low sea levels of the late Miocene (Fig. 2). An early migration (M1) occurred 8.5 to 5.6 Ma when a progenitor of the caracal lineage arrived in Africa. The

second migration (M2) relocated a common ancestor to five felid lineages (ocelot, lynx, puma, leopard cat, and domestic cat) across the Bering land bridge to North America for the first time, 8.5 to 8.0 Ma (Fig. 2). This New World migration (M2) would be coincident with a period when a rich assemblage of Eurasian carnivores (ursid, procyonid, mustelid, and saber-toothed felid species) is postulated to have crossed from Eurasia to North America (19) and would precede the differentiation of the ocelot, puma, and lynx lineages 8.0 to 6.7 Ma (Fig. 1). The divergence of the ocelot lineage occurred 8.0 to 2.9 Ma (Table 1, nodes 4 and 23), and further species differentiation was likely facilitated by the Panamanian land bridge 2.7 Ma (M3) and faunal exchange with South America (20). Between 6.7 and 6.2 Ma the domestic cat and leopard cat lineages probably diverged from Eurasian forebears that either had remained in Asia (split off from the New World M2 immigrants) or derived from American migrants that crossed the Bering land bridge (M4), as has been postulated for several Canidae and Camelidae species (21).

Today, four major Felidae lineages occur within zoogeographical regions of their orig-

Table 1. Summary of support values for each of the nodes depicted in Fig. 1, including Bayesian estimated date of divergence, with the corresponding 95% credibility interval, the estimated time before the node, and bootstrap support values for the minimum evolution (ME), maximum parsimony (MP), and maximum likelihood (ML) analyses and Bayesian (BAY) posterior probabilities (9). Bootstrap values <50% are marked (<). Indels that support each node are noted by the gene abbreviation where they occur, the number of base pairs inserted (+) or deleted (–), and an asterisk denoting a possible short tandem repeat element (STR) (table S7). RD114 and FeLV are endogenous retroviral families (10), and *Numt* are large nuclear insertions of mtDNA (11, 12). Y-linked genes are in bold capital letters. Species abbreviations are defined in Fig. 1.

Node	Description of node	Date (Ma)	Confidence interval	Time prior to node (My)	Divtime fossil Constraint (My)	Insertion/deletion variants[2]	nDNA ME	nDNA MP	nDNA ML	nDNA BAY	mt DNA ME	mt DNA MP	mt DNA ML	mt DNA BAY	Total DNA ME	Total DNA MP	Total DNA ML	Total DNA BAY
		Divergence Time (Ma)					Percentage Statistical Support											
1	**Felidae base**	10.78	8.38, 14.45		<16.0		100	100	100	100	100	100	88	100	100	100	100	100
2	Bay cat lineage and node 3	9.43	7.36, 12.77	1.35			82	74	93	100	64	<	70	<	99	100	100	100
3	Caracal lineage and node 4	8.51	6.66, 11.56	0.92		UBE1Y(+2)	85	97	87	100	<	<	<	<	74	50	55	100
4	Ocelot lineage and node 5	8.05	6.30, 10.95	0.46	>5.0		90	79	80	100	<	<	<	<	70	40	55	100
5	Lynx lineage and node 6	7.15	5.62, 9.81	0.90	>5.3	SRY5(-5)*	98	97	99	100	<	<	<	<	92	72	94	100
6	Puma lineage and node 7	6.70	5.27, 9.20	0.45			<	56	59	99	<	<	<	<	<	<	55	<
7	nodes 8 and 14	6.18	4.80, 8.55	0.52	>4.2		100	99	99	100	<	69	<	100	100	96	100	100
8	**Domestic cat lineage**	3.36	2.41, 4.88	2.82		SMCY(+SINE), UBE1Y(+2)*, RD114, FeLV	100	100	100	100	100	100	100	100	100	100	100	100
9	(Fni, Fma, Fca, Fsi, Fli, Fbi)	3.04	2.16, 4.44	0.32		SRY5(-9), *Numt* insert1	<	76	75	65	<	<	<	<	<	<	<	100
10	(Fma, Fca, Fsi, Fli, Fbi)	2.49	1.72, 3.67	0.55	>1.0		99	98	99	100	100	100	100	100	100	100	100	65
11	(Fca, Fsi, Fli, Fbi)	1.40	0.89, 2.16	1.09			100	100	100	100	<	100	89	100	100	100	100	100
12	(Fca, Fsi)	0.99	0.59, 1.62	0.41			62	<	54	63	<	<	<	<	<	<	<	<
13	(Fli, Fbi)	1.17	0.72, 1.86	0.23			76	68	68	100	<	<	<	<	<	<	<	<
14	**Leopard cat lineage**	5.86	4.53, 8.16	0.32	>1.0	APP(+1)	93	76	83	100	<	<	<	<	<	<	<	83
15	(Pru, Pbe, Pvi, Ppl)	4.59	3.42, 6.54	1.27		CLU(+2)	99	100	100	100	69	100	100	100	100	100	100	100
16	(Pbe, Pvi, Ppl)	2.94	2.04, 4.31	1.65		CLU(-1)	100	100	100	100	99	98	99	100	100	100	100	100
17	(Pvi, Ppl)	2.55	1.74, 3.82	0.39			81	72	72	100	100	100	100	100	100	100	100	100
18	**Puma lineage**	4.92	3.86, 6.92	1.78	>3.8		100	100	100	100	73	<	55	100	100	100	100	100
19	(Pco, Pya)	4.17	3.16, 6.01	0.75	>1.8	DGKG(-4)*, CLU(-1)*	99	100	100	100	<	<	<	56	78	94	100	100
20	**Lynx lineage**	3.24	2.53, 4.74	3.93	>2.5	CLU(-1), GNB(-1), ALAS(-2)*, **ZFY(-6)**	100	100	100	100	98	99	99	100	100	100	100	100
21	(Lca, Lyp, Lly)	1.61	1.06, 2.60	1.63			100	100	100	100	100	100	100	100	100	100	100	100
22	(Lyp, Lly)	1.18	0.70, 1.98	0.43			<	92	84	100	54	<	<	<	<	<	56	100
23	**Ocelot lineage[1]**	2.91	2.02, 4.25	5.15	<5.0	CLU(-1), DGKG(-3), GNB(-1), TCP (-1), TCP(+6)	100	100	100	100	100	100	99	100	100	100	100	100
24	(Lpa, Lwi)	1.58	1.01, 2.41	1.43			84	68	99	100	100	100	<	100	<	<	54	100
25	(Lja, Lco, Lti, Lge, Lgu)	2.43	1.68, 3.56	0.48	>1.0		100	99	<	100	98	52	100	100	100	100	100	100
26	(Lja, Lco)	1.80	1.18, 2.70	0.14			98	80	<	100	63	<	<	100	<	<	<	100
27	(Lti, Lge, Lgu)	0.93	0.56, 1.48	1.01			<	100	100	100	<	<	<	<	97	80	99	100
28	(Lge, Lgu)	0.74	0.41, 1.21	0.19		GNB(-3)*	75	96	90	100	100	100	100	100	100	100	100	100
29	**Caracal lineage**	5.59	4.14, 7.91	2.93	>3.8	CLU(+1), CLU(+1), **SMCY(-4)**	100	100	100	100	80	86	77	100	100	100	100	100
30	(Cca, Cau)	1.88	1.19, 2.93	3.71		GNB(-3), RASA(-3)*, **UBE1Y(-4)**	100	100	100	100	100	100	100	100	100	100	100	100
31	**Bay cat lineage**	5.86	4.27, 8.42	3.57		**PLP(+1), UBE1Y(-18)**	100	100	100	100	<	<	<	<	100	100	100	100
32	(Pba, Pte)	4.30	2.96, 6.42	1.56			<	100	100	100	100	100	100	100	100	100	100	100
33	**Panthera lineage**	6.37	4.47, 9.32	4.41	>3.8	**SRY3(+4)**, *Numt* insert 2	100	100	100	100	58	100	100	100	100	100	100	100
34	(Ple, Pon, Ppa, Pti, Pun)	3.72	2.44, 5.79	2.65		**SRY3(-7)**	100	100	100	100	64	100	100	100	100	100	100	100
35	(Ple, Pon, Ppa)	2.87	1.81, 4.63	0.85			90	88	93	100	<	<	<	<	<	<	68	100
36	(Ple, Pon)	2.06	1.22, 3.46	0.81			68	77	78	100	<	<	<	99	<	<	<	100
37	(Pti, Pun)	2.88	1.82, 4.62	0.84	>1.0		99	92	92	100	<	<	76	<	100	99	100	100

[1]The NNI ML search placed Lja basal to the six other species in the lineage, but with a lower score (-ln 66463.95 versus 66459.92), as did the ME and MP analyses.   [2]Indel variants are indicated in combined alignment of all gene segments in figure S2.

REPORTS

inal establishment: the bay cat and leopard cat lineages (Oriental), the caracal lineage (Ethiopian), and the ocelot lineage (Neotropical) (Figs. 1 and 2). The other lineages include species inhabiting different continents, supporting the premise of six additional Pliocene/Pleistocene migrations (M5 to M10). Among them was the cheetah, which originated in the North American puma lineage (Fig. 1) and migrated to central Asia and Africa (M5). Similarly, progenitors of the Eurasian and Iberian lynxes migrated across the Bering peninsula to Eurasia 1.6 to 1.2 Ma (M6). Further, Asian-derived *Panthera* species spread into America (jaguar-M7 and lion-M8) and into Africa (lion and leopard-M9) (*22*). Our proposed scenario would also require Pleistocene migrations into Africa of the sand cat, black-footed cat, and African wild cat (M10). More temperate climates and substantially lower sea levels associated with major Pleistocene glaciations facilitated several other faunal movements between North America and Asia during this period, including pulses of dispersal by microtine rodents (*21*) and humans (*23*).

Modern felids examined to date have relatively recent coalescent dates (*24*).

Although we employ 16 fossil dates (*9*), estimated molecular dates (Table 1) reveal large portions of felid history for which the fossil record is incomplete. By identifying the oldest fossil for every branch on the tree and comparing it with the Bayesian estimated molecular divergence date for that branch (table S6 and fig. S12), we estimated the average unrepresented basal branch length (UBBL) (*25*). This analysis indicated that the fossil record underestimates the first age of evolutionary divergences along each evolutionary branch on average by 76% or by 73% for the terminal branches and 79% for the internal branches. These figures are comparable to those derived for bats (Chiroptera) (*25*) and support the perception that a large portion of felid evolutionary history is not represented in the fossil record.

Our combined data set resulted in a fairly well resolved phylogenetic tree, but as in Rokas *et al*. (*26*), specific subsets of the data seldom produced comparable resolution or statistical support (figs. S1 to S11 and table S4).

Of the four main genetic data groups, mtDNA was the most divergent, followed by yDNA. There were 1175 mtDNA parsimony informative sites (PI) among felids and 838 nDNA PI (443 aDNA, 279 yDNA, and 116 xDNA PI) (table S1). Despite the comparatively larger amount of data (and signal) (table S5), overall mtDNA variation was least robust in node resolution with a high mtDNA homoplasy index (HI) (0.705), compared with aDNA (0.197), xDNA (0.111), and yDNA (0.114). The 4456 bp of yDNA and the 11,166 bp of aDNA did the best at distinguishing the eight major lineages (eight of eight with >97% ML BS), whereas mtDNA genes (3936 bp) provided >80% ML BS for only four of these eight lineages. The yDNA genes also provided the most shared derived sites defining each lineage and the relative order of lineages (four of seven nodes with >83% ML BS) (*9*).

The evolutionary time frame and phylogenetic challenges for the Felidae are analogous to those encountered in great ape studies [e.g., (*27*, *28*)], in which, for example, only 60% of the phylogenetically informative sites or loci supported a generally accepted human/chimpanzee clade, whereas the remaining 40% supported alternative arrangements (*29*). Within the felid phylogeny, 21 of the 36 divergences occurred in less than 1.0 million years, and the seven basal nodes are spaced an average 600,000 years apart. Similar radiations are common throughout mammalian evolutionary history, which suggests that confident resolution of these will also require large, multigenic data sets.
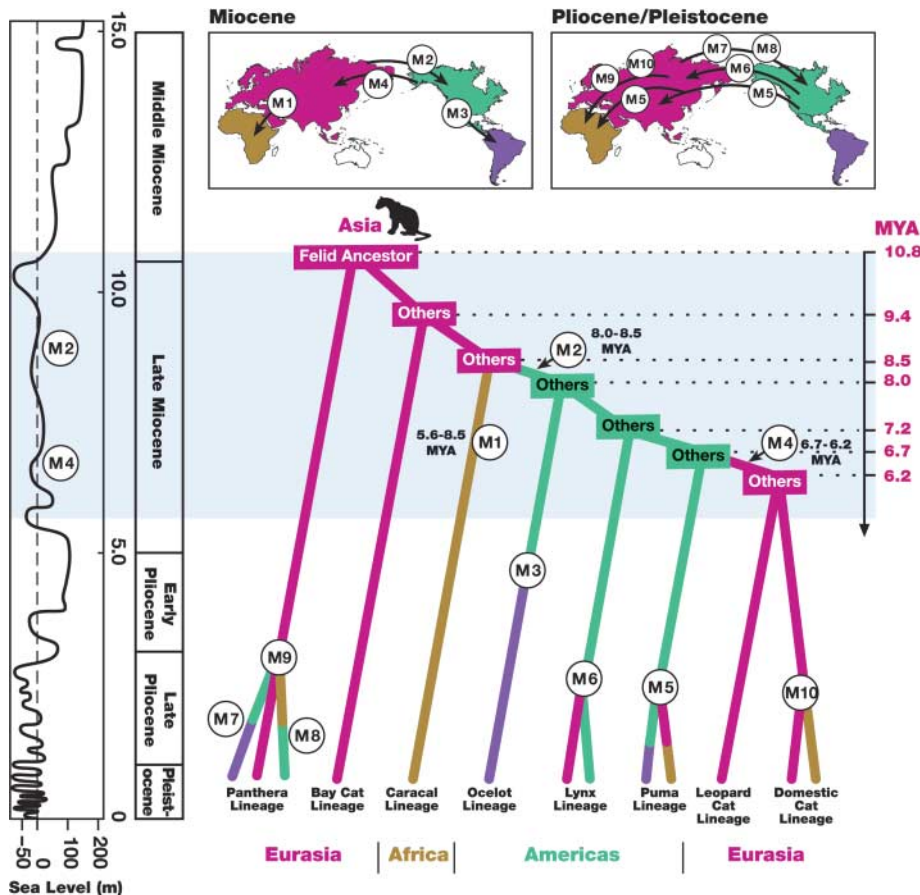

Fig. 2. A depiction of hierarchical divergence, estimated dates, and inferred intercontinental migrations along the phylogenetic lineages in Fig. 1 imputed from Bayesian dating, phylogenetic analyses, the fossil record, current species distributions, and an analysis of possible migration scenarios (*9*). Deduced intercontinental migrations (M1 to M10) and correspondence with major changes in worldwide sea levels, as depicted on a eustatic sea-level curve (on left) [modified from (*16*)], are described in the text.

References and Notes

1. K. Nowell, P. Jackson, *Status Survey and Conservation Action Plan, Wild Cats* (International Union for Conservation of Nature and Natural Resources, Gland, Switzerland, 1996).
2. R. M. Nowak, *Walker's Mammals of the World* (Johns Hopkins Univ. Press, Baltimore, MD, 1999).
3. M. C. McKenna, S. K. Bell, *Classification of Mammals Above the Species Level* (Columbia Univ. Press, NY, 1997).
4. L. O. Salles, *Am. Mus. Novit.* **3047**, 1 (1992).
5. M. C. Mattern, D. A. McLennan, *Cladistics* **16**, 232 (2000).
6. W. E. Johnson, S. J. O'Brien, *J. Mol. Evol.* **44**, S98 (1997).
7. J. Pecon-Slattery, S. J. O'Brien, *Genetics* **148**, 1245 (1998).
8. J. Pecon-Slattery, A. J. Pearks Wilkerson, W. J. Murphy, S. J. O'Brien, *Mol. Biol. Evol.* **21**, 2299 (2004).
9. Materials and methods are available as supporting material on *Science* Online and the Laboratory of Genomic Diversity, NCI, Web site, http://home.ncifcrf.gov/ccr/lgd.
10. R. E. Benveniste, in *Molecular Evolutionary Genetics, Monographs in Evolutionary Biology Series,* R. J. MacIntyre, Ed. (Plenum Press, New York, 1985), pp. 359–417.
11. J. V. Lopez, N. Yuhki, R. Masuda, W. Modi, S. J. O'Brien, *J. Mol. Evol.* **39**, 174 (1994).
12. J. Kim *et al.*, *Gene*, in press.
13. A. D. Yoder *et al.*, *Nature* **421**, 734 (2003).
14. P. Gaubert, G. Veron, *Proc. R. Soc. London Ser. B. Biol. Sci.* **270**, 2523 (2003).
15. G. de Beaumont, *Eclogae Geologicae Helvetiae* **57**, 837 (1964).
16. B. U. Haq, J. Hardenbol, P. R. Vail, *Science* **235**, 1156 (1987).
17. R. M. Hunt, in *Carnivore Behavior, Ecology, and Evolution, Vol. 2*, J. L. Gittleman, Ed. (Cornell Univ. Press, Ithaca, NY, 1996), pp. 485–541.
18. D. S. Woodruff, *J. Biogeogr.* **30**, 551 (2003).
19. Q. Zhanxiang, *Bull. Am. Mus. Nat. Hist.* **279**, 163 (2003).

20. L. G. Marshall, *Am. Sci.* **76**, 380 (1988).
21. C. A. Repenning, *Quat. Sci. Rev* **20**, 25 (2001).
22. L. Werdelin, M. E. Lewis, *Zool. J. Linn. Soc.* **144**, 121 (2005).
23. P. Forster, *Philos. Trans. R. Soc. London Ser. B* **359**, 255 (2004).
24. S. J. O'Brien, W. E. Johnson, *Annu. Rev. Genet. Hum. Genet.* **6**, 407 (2005).
25. E. C. Teeling *et al.*, *Science* **307**, 580 (2005).
26. A. Rokas, B. L. Williams, N. King, S. B. Carroll, *Nature* **425**, 798 (2003).
27. Z. Yang, *Genetics* **162**, 1811 (2002).
28. G. V. Glazko, M. Nei, *Mol. Biol. Evol.* **20**, 424 (2003).
29. C. O'hUigin, Y. Satta, N. Takahata, J. Klein, *Mol. Biol. Evol.* **19**, 1501 (2002).
30. Content of this publication does not necessarily reflect views or policies of the Department of Health and Human Services. A.A. received a Fundação para a Ciência e Tecnologia grant (SFRH/BPD/5700/2001). This research was supported by federal funds from the NIH/NCI (N01-CO-12400) and the NIH/NCI/CCR Intramural Research Program.

Alterations in 5-HT$_{1B}$ Receptor Function by p11 in Depression-Like States

Per Svenningsson,[1,2] Karima Chergui,[2] Ilan Rachleff,[1] Marc Flajolet,[1] Xiaoqun Zhang,[2] Malika El Yacoubi,[3] Jean-Marie Vaugeois,[3] George G. Nomikos,[4] Paul Greengard[1]*

The pathophysiology of depression remains enigmatic, although abnormalities in serotonin signaling have been implicated. We have found that the serotonin 1B receptor [5-hydroxytryptamine (5-HT$_{1B}$) receptor] interacts with p11. p11 increases localization of 5-HT$_{1B}$ receptors at the cell surface. p11 is increased in rodent brains by antidepressants or electroconvulsive therapy, but decreased in an animal model of depression and in brain tissue from depressed patients. Overexpression of p11 increases 5-HT$_{1B}$ receptor function in cells and recapitulates certain behaviors seen after antidepressant treatment in mice. p11 knockout mice exhibit a depression-like phenotype and have reduced responsiveness to 5-HT$_{1B}$ receptor agonists and reduced behavioral reactions to an antidepressant.

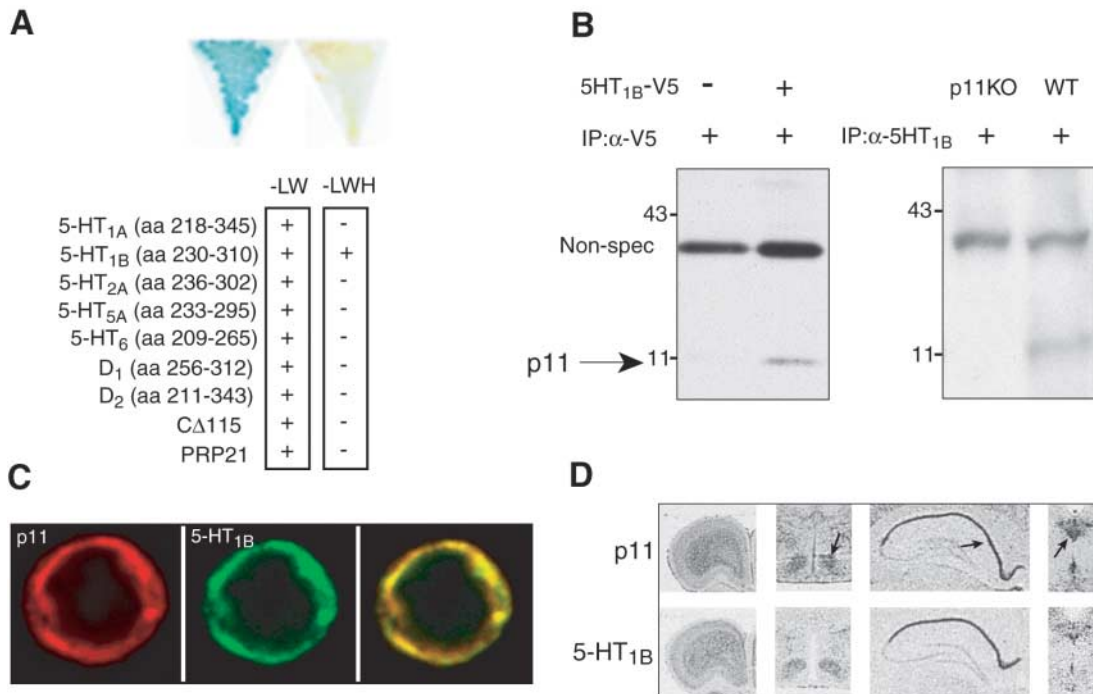The serotonin system plays a key modulatory role in a plethora of functions of the central nervous system in physiological and disease states (*1*, *2*). Compounds that alter either the reuptake or the metabolism of serotonin are used as medications against many neuropsychiatric disorders (*1–4*). A better understanding of the role of individual serotonin receptors in mediating the effects of these medications would improve our comprehension of the etiology of certain neuropsychiatric disease states and enhance our ability to design more effective medications. There are 14 different serotonin receptors (*2*), some of which have multiple splice variants that enable binding of distinct sets of intracellular proteins (*5*). 5-HT$_{1B}$ receptors play a crucial role in regulating serotonin neurotransmission, as they serve as both autoreceptors on serotonin-containing neurons originating from the raphe nuclei and heteroreceptors on several neurons that do not

[1]Laboratory of Molecular and Cellular Neuroscience, The Rockefeller University, New York, NY 10021, USA. [2]Department of Physiology and Pharmacology, Karolinska Institute, Stockholm, Sweden. [3]Unite de Neuropsychopharmacologie Experimentale—CNRS FRE2735, European Institute for Peptide Research (IFRMP 23), Faculty of Medicine and Pharmacy, Rouen F76183 Cedex, France. [4]Neuroscience Discovery Research, Eli Lilly and Company, Lilly Corporate Center, Indianapolis, IN 46285, USA.

*To whom correspondence should be addressed, E-mail: greengard@rockefeller.edu

Fig. 1. Identification of an interaction between 5-HT$_{1B}$ receptors and p11. (**A**) Results from a yeast two-hybrid screen showing an interaction of p11 with the 5-HT$_{1B}$ receptor (left; blue color), but not with an unrelated bait (CΔ115; right; no color), or with pRP21, 5-HT$_{1A}$, 5-HT$_{2A}$, 5-HT$_{5A}$, 5-HT$_6$, D$_1$, or D$_2$ receptors. (**B**) Coimmunoprecipitation confirming that p11 interacts with (left panel) V5 epitope–tagged 5-HT$_{1B}$ receptors in HeLa cells and with (right panel) native 5-HT$_{1B}$ receptors in brain tissue from wild-type, but not p11 KO, mice. The immunoprecipitates were analyzed by Western blotting using a p11-specific antibody. The nonspecific band corresponds to the light chains of the antibodies against V5 or 5-HT$_{1B}$ receptors (α-V5 and α-5HT$_{1B}$). (**C**) Immunofluorescence staining of p11 (left, red fluorescence), V5 epitope–tagged 5-HT$_{1B}$ receptors (middle, green fluorescence) and their colocalization (right, yellow fluorescence) at the cell surface in HeLa cells. (**D**) In situ hybridization made on coronal sections from a rat brain showing that the distribution of p11 mRNA is similar to that of 5-HT$_{1B}$ receptor mRNA in (left to right) frontal cortex, ventromedial hypothalamus (arrow), hippocampus (arrow), and raphe nuclei (arrow).